

# Characterising the influence of milk fat towards an application for extrusion-based 3D-printing of casein–whey protein suspensions via the pH–temperature-route

Daffner, Kilian; Ong, Lydia; Hanssen, Eric; Gras, Sally; Mills, Tom

DOI:

[10.1016/j.foodhyd.2021.106642](https://doi.org/10.1016/j.foodhyd.2021.106642)

License:

Creative Commons: Attribution-NonCommercial-NoDerivs (CC BY-NC-ND)

*Document Version*

Peer reviewed version

*Citation for published version (Harvard):*

Daffner, K, Ong, L, Hanssen, E, Gras, S & Mills, T 2021, 'Characterising the influence of milk fat towards an application for extrusion-based 3D-printing of casein–whey protein suspensions via the pH–temperature-route', *Food Hydrocolloids*, vol. 118, 106642. <https://doi.org/10.1016/j.foodhyd.2021.106642>

[Link to publication on Research at Birmingham portal](#)

## General rights

Unless a licence is specified above, all rights (including copyright and moral rights) in this document are retained by the authors and/or the copyright holders. The express permission of the copyright holder must be obtained for any use of this material other than for purposes permitted by law.

- Users may freely distribute the URL that is used to identify this publication.
- Users may download and/or print one copy of the publication from the University of Birmingham research portal for the purpose of private study or non-commercial research.
- User may use extracts from the document in line with the concept of 'fair dealing' under the Copyright, Designs and Patents Act 1988 (?)
- Users may not further distribute the material nor use it for the purposes of commercial gain.

Where a licence is displayed above, please note the terms and conditions of the licence govern your use of this document.

When citing, please reference the published version.

## Take down policy

While the University of Birmingham exercises care and attention in making items available there are rare occasions when an item has been uploaded in error or has been deemed to be commercially or otherwise sensitive.

If you believe that this is the case for this document, please contact [UBIRA@lists.bham.ac.uk](mailto:UBIRA@lists.bham.ac.uk) providing details and we will remove access to the work immediately and investigate.

**Characterising the influence of milk fat towards an application for extrusion-based 3D-printing of casein–whey protein suspensions via the pH–temperature-route**

Kilian Daffner <sup>a</sup>, Lydia Ong <sup>b,c</sup>, Eric Hanssen <sup>d,e</sup>, Sally Gras <sup>b,c,e</sup>, Tom Mills <sup>a</sup>

<sup>a</sup> Department of Chemical Engineering, University of Birmingham, Edgbaston, Birmingham B15 2TT, United Kingdom

<sup>b</sup> The ARC Dairy Innovation Hub, The University of Melbourne, Parkville, Victoria, 3110, Australia

<sup>c</sup> Department of Chemical Engineering, The University of Melbourne, Parkville, Victoria, 3010, Australia

<sup>d</sup> Advanced Microscopy Facility, The Bio21 Molecular Science and Biotechnology Institute, The University of Melbourne, Parkville, Victoria, 3010, Australia

<sup>e</sup> Department of Biochemistry and Molecular Biology, The University of Melbourne, Parkville, Victoria, 3010, Australia

Corresponding author: Kilian Daffner

E-mail address: KXD744@bham.ac.uk

---

**Keywords:** food printing, acidified milk gels, protein–fat suspension, heat-induced gelation, physical properties

## ABSTRACT

This study presents the design and characterisation of casein–whey protein suspensions (8.0/10.0% (w/w) casein and 2.0/2.5% (w/w) whey protein) mixed with dairy fat (1.0, 2.5 and 5.0% (w/w) total fat) processed via the pH–temperature-route in preparation for 3D-printing. Mechanical treatment was applied to significantly decrease the particle size of the milk fat globules and increase surface area, creating small fat globules ( $< 1\ \mu\text{m}$ ) covered with proteins, which could act as pseudo protein particles during gelation. Different proteins covered the fat globule surface after mechanical treatment, as a result of differences in the pH adjusted just prior to heating (6.55, 6.9 or 7.1). The protein-fat suspensions appeared similar by transmission electron cryogenic microscopy and the zeta-potential of all particles was unchanged by the heating pH, with a similar charge to the solution ( $\sim -20\ \text{mV}$ ) occurring after acidification (pH 4.8/5.0) at low temperatures ( $2^\circ\text{C}$ ). A low heating pH (6.55) resulted in increased sol–gel transition temperatures ( $G' = 1\ \text{Pa}$ ) and a decreased rate of aggregation for protein–fat suspensions. A higher heating pH (6.9 and 7.1) caused an increased rate of aggregation (aggregation rate  $\geq 250\ \text{Pa}/10\ \text{K}$ ), resulting in materials more promising for application in extrusion-based printing. 3D-printing of formulations into small rectangles, inclusive of a sol–gel transition in a heated nozzle, was conducted to relate the aggregation rate towards printability.

## 1 Introduction

3D-printing, or additive manufacturing (AM), is a robotic construction technology that deposits materials layer-by-layer to build a three-dimensional object and that gains more and more interest in the area of foods (Wegrzyn, Golding, & Archer, 2012). 3D-printing of food, or food layered manufacturing (FLM), has been recently used to print a different range of food grade materials, including chocolate (Lanaro et al., 2017), hydrocolloid-based materials (Gholamipour-Shirazi et al., 2019) or processed cheese (Le Tohic et al., 2017), although the first food being printed was already in 2006 (Malone & Lipson, 2006). This printing technology offers advantages such as individualised products, flexibility with respect to nutritional content, and also the potential to reduce waste and storage or distribution costs of the final product compared to conventional mass production of food (Godoi, Prakash, & Bhandari, 2016; Ross, Kelly, & Crowley, 2019).

While the actual printing of food and post-characterisation following printing has received considerable attention, few experiments have considered defining the desirable material properties for optimal printing (Derossi, Caporizzi, Azzollini, & Severini, 2018). Food grade materials have complex nano- and microstructure, as well as altered properties associated with solid to liquid phase transition, complicating their use in printing. A greater understanding of the material properties will enable the design of useful formulations and is perhaps of one the most important steps in the printing of a range of edible foods. Edible and printable formulations need to match several requirements. For example, they should ideally be of homogenous composition, have suitable flow properties and enable printability in a layer-by-layer manner (Godoi et al., 2016; Kim, Bae, & Park, 2017).

There is a high demand for fermented concentrated dairy products, rich in protein and fat, such as Greek yogurt or fresh cheese (Jørgensen et al., 2019), and FLM has the potential to produce dairy-based products for tailored nutrition. Nöbel, Seifert, Schäfer, Daffner and Hinrichs (2018)

were the first to implement a pH–temperature (T)-route, including cold acidification followed by heating, for printing of milk concentrates inclusive of a sol–gel transition, which resulted in small printed spheres. For the pH–T-route, direct acidification at cold temperatures ( $\leq 10^{\circ}\text{C}$ ) to pH values approaching the isoelectric point (IEP) of casein (4.6) helped to maintain solution (sol)–characteristics due to a reduction of hydrophobic interaction forces (Horne, 1998). Increased temperatures then resulted in increasing hydrophobic interaction forces and particle aggregation (Hammelehle, 1994; Roefs, 1986; Schäfer et al., 2018). Pre-chilled acidified concentrates from milk microfiltration differing in pH (4.8 – 5.4) and casein content (8.0 – 12.0% (w/w)) have also been investigated and characterised for their suitability for 3D-printing (Nöbel et al., 2018; Nöbel, Seifert, Schäfer, Daffner, & Hinrichs, 2020). Formulations at pH 4.8 formed firm and homogeneous milk gels when printed. In contrast, the milk gels at pH 5.0 were not mechanically stable after printing, illustrating the importance of pH as a process variable to alter printed food properties.

Recently, casein–whey protein suspensions differing in their protein content, acidification - and the pH at which heating was conducted were also characterised via the pH–T-route (Daffner et al., 2020a). It would be of high interest to see whether dairy fat could be added to such formulations and how this would change the microstructure and suitability of the dairy-based feedstock regarding printing. It is established that the rheological behaviour of dairy products like cheese, yoghurt or mayonnaise is influenced by the presence of emulsified fat (Dickinson, 2012). Mechanical input causes oil droplets being covered and stabilised by a thin layer of proteins adsorbed at the oil–water interface (Dickinson, 1994). During high pressure homogenisation, CM and casein molecules also adsorb at the surface of the newly created milk fat globule membrane (MFGM), sterically and electrostatically stabilising the droplets against re-coalescence (McClements, 2004). Homogenisation has also been shown to cause milk fat globules (MFG) to behave to some extent like CM (Buchheim, 1986).

91 The surface properties are a further characteristic of the MFG that can influence printability.  
92 The zeta ( $\zeta$ )-potential of MFG is reported to be around  $-13.5$  mV (Michalski, Michel, Sainmont,  
93 & Briard, 2002a), with the MFGM phospholipids having a similar potential of  $-13$  mV (Liu,  
94 Ye, Liu, Liu, & Singh, 2013). This  $\zeta$ -potential increases to around  $-20$  mV for homogenised  
95 MFG due to CM covering the newly created surface, approaching the  $\zeta$ -potential of the protein  
96 casein. These results led to the assumption that the electrophoretic mobility of casein in the  
97 serum and casein adsorbed on the surface of the MFG were the same (Michalski et al., 2002a).  
98 When included in dairy gels, the MFG with a surface covered by casein and whey protein causes  
99 an increase in firmness, essentially increasing the apparent protein concentration (Aguilera &  
100 Kessler, 1988; Hammelehle, 1994; Ji et al. 2016; Van Vliet & Dentener-Kikkert, 1982).

101 MFG with protein on the surface were shown to act as pseudo-protein particles during gelation  
102 and increase gel firmness (Ji, Lee, & Anema, 2016). The aim of this study was to develop novel  
103 printable formulations for tailored nutrition by adding dairy fat to casein–whey protein suspen-  
104 sions for application in extrusion-based FLM via the pH–T-route. Adjusting the pH before  
105 heating was expected to cause a change in the types of protein covering the surface of the MFG  
106 after mechanical input. We hypothesise that this change in the surface properties of the MFG  
107 influences the overall formulation characteristics, tailoring the sol–gel transition temperature  
108 and manipulating the aggregation rate, with the latter property recently related towards printa-  
109 bility (Daffner et al., 2020a). Several parameters including the protein and the fat content, as  
110 well as the pH during heating and cold acidification, were adjusted to design and characterise  
111 novel formulations towards printing applications.

## **2 Material and Methods**

### **2.1 Material**

Micellar casein concentrate (MCC 85) and German Prot 9000 - Whey protein isolate (WPI) were provided by Sachsenmilch Milk & Whey Ingredients (Sachsenmilch Leppersdorf GmbH, Wachau, Germany). The manufacturer specifications are provided in Daffner et al. (2020a). Cream (dairy fat) was bought from a local supermarket (Sainsbury's, Birmingham, UK) and 100 mL contained 47.5% (w/w) fat, 1.5% (w/w) lactose, 1.5% (w/w) protein and 0.05% (w/w) salt. For pH adjustment, citric acid (1M) (Sigma Aldrich, UK) was prepared in Milli-Q water (Elix® 5 distillation apparatus, Millipore®, USA) and sodium hydroxide (1M) was bought from Sigma Aldrich (UK).

### **2.2 Sample preparation**

Casein–whey protein suspensions (4:1 ratio, casein to whey protein) were prepared following the procedure of Daffner et al. (2020a). After a full hydration of the proteins overnight, fat was added to the protein suspensions (with a starting pH of  $6.7 \pm 0.1$ ) to obtain final fat concentrations of 1.0, 2.5 or 5.0% (w/w). Before the heat treatment, the pH was adjusted to 6.55 (with 1 M citric acid) or either 6.9 or 7.1 (with 1 M NaOH). The protein–fat suspensions were indirectly heated in a water bath on a stirring plate at 80°C for 10 min to ensure denaturation of the whey proteins (degree of denaturation  $\beta$ -LG  $\geq 80\%$ ; estimated from Kessler, 2002). After heating, the protein–fat suspensions were subjected to pre-homogenisation at  $50.0 \pm 2.0^\circ\text{C}$  using a high intensity ultrasonic vibracell processor (Vibra Cell 750, Sonics, USA) operating in a continuous mode, at 750 W and 20 kHz. The power output was set at 95% of the nominal power and sonication was conducted for 2 min, with 4 seconds on and 2 seconds off (3 min in total). Directly after pre-homogenisation, each sample was passed through a high-pressure valve homogeniser (Panda NS1001L-2K, Gea Niro Soavi, Parma, Italy) at 500 bars and  $50.0 \pm 2.0^\circ\text{C}$ . All formulations were cold acidified at 2°C to pH values of 4.8 or 5.0, as described in Daffner et al. (2020a).

## **2.3 Rheology**

Rheological measurements were conducted by a Kinexus Pro rheometer (Malvern Instruments, UK) with a cup ( $D = 27.17$  mm, depth = 63.5) and vane ( $d = 61$  mm, height = 25 mm)-geometry. For dynamic oscillatory measurements, temperature sweeps were performed from 2 – 60°C with a heating rate of 1 K/min, following the procedure of Daffner et al. (2020a). The sol–gel transition temperature was determined when  $G'$  reached a value of 1 Pa (Daffner et al., 2020a; Nöbel et al., 2018; Nöbel et al., 2020; Schäfer et al., 2018).

## **2.4 Zeta-potential and particle size measurements**

The particle size and the zeta ( $\zeta$ )-potential were determined using a Mastersizer 2000 (Malvern Instruments, UK) and a Zetasizer (Malvern Instruments, UK). A drop of the untreated dairy fat was placed into the circulating cell which contained deionised water and the particles in the micro range were measured at 20°C. Refraction indices of 1.46 and 1.33 were set for milk fat and water respectively. After homogenisation, the Zetasizer was used to characterise the formulations to give particle size distribution in the nanometre range. Samples were diluted 100 times with deionised water before experiments and  $\zeta$ -potential measurements were performed over a range of pH values (6.8 to 4.8), as described in Daffner et al. (2020a).

## **2.5 Microscopy**

### **2.5.1 CLSM**

#### **2.5.1.1 Preparation of samples**

Thermally and mechanically treated protein–fat suspensions were prepared for CLSM, mainly following the procedure of Ong, Dagastine, Kentish, & Gras (2010a). A volume of 10  $\mu$ l of each of fast green FCF solution (1 mg/ml in MilliQ water, Sigma-Aldrich, St. Louis, U.S.A.) and Nile red solution (1 mg/ml in 100% dimethyl sulfoxide, Sigma-Aldrich, St. Louis, U.S.A.) was added to 480  $\mu$ l of the sample that included protein and fat particles. The stained sample was diluted 1:5 with agarose solution (40°C, 0.25g/50 ml Milli Q water) to reduce particle



movement due to Brownian motion, as shown in previous literature (Lopez, Madec, & Jimenez-Flores, 2010; Devnani, Ong., Kentish, & Gras, 2020). The fat specific stain Nile red only stained the fat core of the MFG and did not provide any information about the MFGM (Ong et al., 2010a). According to the procedure of Ong et al. (2010a), a 10  $\mu$ l aliquot of the stained sample was transferred to a cavity slide (0.7 mm in depth) (ProSciTech, Thuringowa, Australia), covered with a glass coverslip (0.17 mm thick) and secured with nail polish (Maybelline LLC, U.S.A.). The sample was then inverted for analysis by CLSM.

#### **2.5.1.2 CLSM**

The microstructure of the samples was observed using an inverted confocal scanning laser microscope (Leica SP8; Leica Microsystems, Heidelberg, Germany) powered by Ar/Kr and He/Ne lasers. All samples were viewed using an oil immersion 63 x lens (1.32 Numerical Aperture) and the pinhole diameter was maintained at 1 Airy Unit. All the wavelengths were adjusted according to Ong et al. (2010a).

#### **2.5.1.3 Image analysis of CLSM micrographs**

Image analysis of CLSM micrographs was performed with LAS X software (LAS X Core Offline version for Life Science, Leica Microsystems). Images were restored by a deconvolution process conducted with Huygens Essential 3.7 software (Scientific Volume Imaging, Netherlands).

#### **2.5.2 Cryogenic transmission electron microscopy and image analysis**

Thermally (80°C, 10 min; adjusted pH 6.55/ 6.9/ 7.1) and mechanically (sonication and homogenisation) treated protein–fat suspensions were prepared for cryo-EM, following the protocol of Daffner et al. (2020b). Samples were diluted 1:10 with deionised water to ensure an optimal number of particles for imaging. Next, a Formvar lacey carbon film mounted on a 300 mesh copper grids (ProSciTech, Australia) was glow discharged to have a hydrophilic support on which the samples (3  $\mu$ l) were adsorbed. To freeze the sample the grids were then plunged in

liquid ethane using a Vitrobot (FEI Company, Eindhoven, Netherlands). The grids were observed on a Tecnai G2 F30 (FEI Company, Eindhoven, Netherlands) operating at 200 kV with no objective aperture, equipped with a CETA CMOS 4kx4k detector (FEI company, Eindhoven, Netherlands). A series of micrographs of increasing dose was recorded for all samples with a defocus value of  $-6.66\ \mu\text{m}$ . High pass filtering and differentiation of the fat and protein particles was performed as described in Daffner et al. (2020b).

## **2.6 SDS-PAGE**

### **2.6.1 Separation and washing of the MFG surface proteins**

The proteins on the surface of the MFG after thermal and mechanical treatment were analysed via SDS-PAGE following the isolation procedure of Sharma, Singh, & Taylor (1996a/ 1996b) and Ye, Singh, Taylor, & Anema (2002), with a few changes. This procedure involved centrifugation (Thermo Sorvall RC-6-Plus; Thermo Scientific, Asheville, USA) of the samples to recover the cream layer first, followed by a washing step to remove serum proteins, and determination of the different types of casein and whey protein covering the fat globule surface layer (Sharma & Dalgleish, 1993). To increase the difference in the density between fat and serum phase, 8.6 g of sucrose was added per 30 g of sample, followed by centrifugation at 18.000 g for 20 min at 20°C to separate the cream. After decanting the supernatant containing excess proteins in solution, not bound to the fat globule membrane, the cream layer at the top of the sample was washed with deionised water and centrifuged at 18.000 g for 20 min at 20°C to remove any further unbound proteins. The washing step was repeated two times, as no further changes in protein content were found when monitoring the supernatant with SDS-PAGE.

### **2.6.2 Isolation and analysis of the fat globule surface protein components**

The identity of the proteins covering the MFG was determined with SDS-PAGE, using precast Bis-Tris 4 – 12/ 12% polyacrylamide gels (Invitrogen, Mulgrave, Victoria, Australia). The

washed cream layers were dispersed (1:25) in a buffer (0.5 M Tris, 2% SDS, 0.5%  $\beta$ -mercaptoethanol, pH adjusted to 6.8) to displace the protein from the FGM (Sharma et al., 1996a). Samples were heated at 90°C for 5 min and centrifuged (2500 g, 20 min, 20°C) to remove the fat from the sample. Subnatants (10  $\mu$ l) were mixed with 5  $\mu$ l NUPAGE 4x LDS sample buffer, 2  $\mu$ l NUPAGE 10x reducing agent containing 0.5 M DTT and 5  $\mu$ l  $\beta$ -mercaptoethanol. Samples were heated (100°C, 3 min) and 10  $\mu$ l of each sample was loaded into the gels. The gels were run, stained, de-stained and visualised as described in Daffner et al. (2020a).

## **2.7 Set-up of a customised 3D-printer**

The retrofitted set-up described in Daffner et al. (2020a) was used for extrusion-based 3D-printing of small rectangles (25 x 25 x 3 mm; 3 layers above each other). A commercially available plastic printer (Crealty Ender 3 Printer; Creality, Shenzhen, China) was customised and used. Before the printing process, the syringe was loaded with 60 ml of the cold acidified protein-fat suspension. To maintain sol-characteristics, a temperature of 2°C was maintained within the syringe cooling jacket. For the formulations to be printed, we followed the temperature-time profiles from another of our previous papers (Nöbel et al., 2020). The temperature of the feedstock before the nozzle was adjusted as follows:  $T_{\text{sol-gel}} - 5\text{K}$  to avoid pre-gelation of the formulations and to ensure a heat-triggered sol-gel transition within the length of the nozzle. Materials were transported via a pipe to the copper nozzle (plastic dye at the end, 1.15 mm in diameter), heated with the heating element and a sol-gel transition was induced. The printing bed was not heated or cooled in this set-up. Printing was performed on a hydrophobic printing paper (10 x 10 cm; Legamaster International B.V., The Netherlands) to prevent spreading of the first layer.

## **2.8 Statistics**

The data plotted in the publication includes the average of at least three measurements accompanied by error bars that consist of the standard deviation of the mean. In the case where mean

values of an observation are compared between samples the data have been subjected to analysis of variance (ANOVA) in order to determine significant differences. Data analysis was conducted with Sigma Plot 12.5 (Systat Software Inc., San Jose, CA, USA). Individual samples were compared with Student's t-test and a level of significance of  $p < 0.05$  was chosen.

## **3 Results**

### **3.1 Physico-chemical characterisation of the sol-state**

The pH-T-route was selected for the creation of promising protein-based formulations with added dairy fat for extrusion-based 3D-printing. Mechanical damage of the MFG in the preparation is necessary to decrease the size and to cover the increased surface area of the MFG with proteins. Previous studies have shown casein and whey proteins to cover more than 40% of the newly created secondary milk fat globule membrane (SFGM), resulting in a significant increase in the storage modulus  $G'$ , shown for acid- and rennet-induced milk gels (Michalski, Cariou, Michel, & Garnier, 2002b). Better gel properties were achieved, if the heating step, which denatures whey proteins, was conducted before the homogenisation step (Hammelehle, 1994), allowing the denatured whey proteins to interact with the MFG, as well as with CM, increasing the number of particles contributing to the overall gelation process.

The goal of this study was to identify if those smaller MFG could behave like CM and actively contribute to the protein-based gelation process as structure promoters (Buchheim, 1986; Ji et al., 2016; Michalski, Michel, & Geneste, 2002c), thereby enhancing printability. The particle size, zeta-potential and surface coverage of the newly created secondary milk fat globule membrane (SDS-PAGE, microscopy), sol-gel transition temperature and aggregation kinetics were investigated, building on a prior study of protein-based systems (Daffner et al., 2020a).

### 3.1.1 Zeta-potential and surface characteristics

Casein–whey protein suspensions were mixed with fat and heated at different pH, treated by mechanical input and then cooled to 2°C, followed by acidification. The  $\zeta$ -potential of the resulting samples is shown in *Fig. 1*, where the data represents an average of all protein and fat particles captured within the sample. An almost linear increase of the  $\zeta$ -potential was found with decreasing pH during acidification and this trend was independent of the pH value before heating. A non-heated micellar casein suspension without any whey protein and fat was also included for comparison (Daffner et al., 2020a).

At an acidification pH of 4.8 and 5.0, the  $\zeta$ -potential of casein–whey protein suspensions with fat was around –20 mV. This demonstrated that sol-characteristics of all formulations, independent of the heating pH, were maintained at an acidification temperature of 2°C and electrostatic repulsion forces between particles were dominant.

A slight trend to lower  $\zeta$ -potential values with increasing heating pH was found. Compared to the pure micellar casein suspensions (non-heated), the addition of fat caused a significant increase in the magnitude of the  $\zeta$ -potential, similar to previous observations (Daffner et al., 2020a). This could be explained by the coverage of the MFG surface with a more complex range of proteins, including CM,  $\kappa$ -casein–whey protein complexes or denatured whey protein (-aggregates) as a result of the pre-processing treatments applied here.

A lower  $\zeta$ -potential between –17 mV to –13 mV was found for MFG in whole milk after homogenisation, dependent on the  $\text{Ca}^{2+}$  concentration (Dalgleish, 1984). For MFG covered with CM after homogenisation at 500 bar, Michalski et al. (2002a) found a similar  $\zeta$ -potential of –20 mV, compared to –13.5 mV for the native MFG. The  $\zeta$ -potential of MFG increased with increasing homogenisation pressure, due to the production of smaller MFG and an increase in surface area covered with more CM. Within their research, they concluded that the  $\zeta$ -potential of a free protein and that of protein adsorbed on a fat globule surface were the same. It was

assumed that the protein charged molecular protuberances on the surface of the carrier were responsible for the mobility of the particles rather than the carrier size (Rajagopalan & Hiemenz, 1997).

### 3.1.2 Particle size distribution

The influence of a mechanical input on the particle size distribution of casein–whey protein suspensions with three different fat contents (1.0% (w/w), 2.5% (w/w) and 5.0% (w/w)) after heating at different pH (6.55, 6.9 and 7.1) is illustrated in *Fig. 2*. The sonication step, followed by high pressure homogenisation caused a significant decrease in the particle size and resulted in a monomodal particle size distribution, with no changes found dependent on the pH at which heating was conducted. The addition of different amounts of fat to protein suspensions had no significant effect on the particle size distribution, although there was a slight tendency to bigger particles with increasing fat content. The z-average of all the particles captured within the protein–fat suspensions was 275 nm (*Fig. 2 inset*), demonstrating a significant increase of 40 – 50 nm in the particle size compared to casein–whey protein suspensions with the same heating pH but without any addition of fat (Daffner et al., 2020a). This larger size results from the fat particles being larger than the protein particles, even after homogenisation.

To intentionally induce a fast, local and irreversible sol–gel transition during printing, the particles need to be within a certain size range; this ensures they will move sufficiently fast to successfully collide and aggregate via the pH–T-route (Daffner et al., 2020a; Nöbel et al., 2018; Nöbel et al., 2020). Formulations with no heat- and mechanical treatment contained large, native and emulsified MFG in the protein suspensions (see *Supplementary Fig. 1*), which slowed down the aggregation and gelation of proteins (data not shown). It is expected that as the size of the MFG approaches the size of the CM, there will be a higher chance that these particles will behave in a similar way (Hammelehle, 1994). It is well known that the rheology of the

overall formulations depends on the behaviour of the continuous phase, if the dispersed particles are well separated from each other and do not aggregate (Dickinson, 1998). In this case, the protein suspension will behave as desired if the MFG are sufficiently small and do not associate.

### **3.1.3 Micrographs from microscopy**

#### **3.1.3.1 CLSM**

CLSM was used to investigate the microstructure of casein–whey protein suspensions mixed with dairy fat after a thermal and mechanical treatment (*Fig. 3*, after heating at pH 7.1) using an intermediate final fat content of 2.5% (w/w). A homogenous distribution of the MFG could be observed in all samples, regardless of the pH adjustment made prior to heating and a representative CLSM image at pH 7.1 is presented in *Fig. 3*. The MFG, stained red in these images, were distributed relatively evenly between the proteins, which were stained green, with the unstained serum phase appearing black in these images. The size of the MFG, which ranges from 50 nm – 1000 nm was consistent with the size of ~275 nm observed by light scattering (*Figure 2*). Protein particles were also found to be adsorbed on the surface of MFG, where they appear as green particles.

Independent of the heating pH, the MFG featured proteins interacting with the membrane surface. After image deconvolution and digital magnification, the proteins covering the surface of the MFG could be better observed (*Fig. 3*, right). Nevertheless, no detailed information of the specific type of protein, protein subunits or aggregates covering the MFG surface could be obtained with this standard confocal microscopy due to the resolution limit of this technique.

#### **3.1.3.2 Cryogenic-EM**

A novel technique was recently described for the more detailed visualisation of interactions between the MFG and the proteins in the hydrated state without chemical fixatives or embedding

(Daffner et al., 2020b). This method of different time-dependent radiation damage allows differentiation between protein (visible damage  $> 150 \text{ e}^-/\text{\AA}^2$ ) and fat (visible damage  $< 25 \text{ e}^-/\text{\AA}^2$ ) particles (Daffner et al., 2020b). Previous studies have observed that the mass of casein and whey protein on the surface of MFG after mechanical and thermal input strongly depended on several parameters including homogenisation pressure, heat treatment and casein-fat ratio (Walstra & Jenness, 1984; Sharma & Dalgleish, 1993; Cano-Ruiz & Richter, 1997). The new cryo technique was therefore applied to assess the presence of proteins on the surface of MFG after the processing techniques applied here.

Proteins were observed on MFG after a heating step applied at different pH (pH 6.55, 6.9 or 7.1) and homogenisation. The images in *Fig. 4* show small spherical MFG ( $\sim 100 \text{ nm}$ ) covered with larger CM and smaller proteins. The proteins were distinguished by increasing the beam exposure. Whilst the proteins were clearly present, no differences were observed in the appearance of these structures for the samples with different heating pH (6.55, 6.9 or 7.1). This observation is consistent with the finding of intact CM covering the MFG surface under similar conditions (heating at  $79^\circ\text{C}$  and a homogenisation pressure of 70 bar), Ye, Anema, & Singh (2008) using the more traditional approach with fixed samples and TEM. The new cryo method is useful for the determination of protein in the hydrated state but does not provide information of the specific type of protein covering the MFG surface. The samples were therefore assessed next by SDS-PAGE analysis.



#### 3.1.4 Analysis of the surface coverage of the MFG via SDS-PAGE

The thermal and mechanical treatment applied in this study reduced the MFG size (see *Fig. 2* and *Fig. 4*) and conversely increased the surface area, allowing proteins to adsorb onto the surface of the smaller MFG. An increase in the pH before heating from 6.55 to 7.1 potentially altered proteins in the samples, without changing the MFG surface area, which may be expected to alter protein composition on the MFG.

An increase in the pH at heating caused an increase in the proportions of  $\alpha$ - and  $\beta$ -casein on the surface of the MFG and only very faint bands of  $\kappa$ -casein and  $\beta$ -LG were detected adsorbed to the surface under these conditions, as shown in *Fig. 5*, where the SDS-PAGE gel shows the protein extracted from the MFG surface and the variation in proteins present for replicate extract samples. Both  $\alpha_{s1}$ - and  $\beta$ -casein have a strong tendency to adsorb at hydrophobic surfaces, due to accessible non-polar residues (Dickinson, 1999) and were expected to preferentially cover the surface of the MFG compared to other proteins, as occurred for all conditions examined here. The increase in casein absorption as a function of pH at heating also led to an increase in the casein–whey protein ratio on the MFG surface from 6.6 to 14.7 as the heating pH was increased, as shown in *Table 1*.

The dissociation of  $\kappa$ -casein from the CM at higher heating pH (6.9, 7.1) has been reported previously (Anema & Klostermeyer, 1997; Daffner et al., 2020a), changing the characteristics of the CM, as well as the aggregates found in the milk serum. This could explain for the preferential adsorption of CM depleted of  $\kappa$ -casein and high in  $\alpha$ - and  $\beta$ -casein observed in this study. This dissociation was also confirmed at higher solids (up to 25%), with increasing pH (6.5 – 7.1) and increasing concentrations causing an increase in the extent of  $\kappa$ -casein dissociation (Singh & Creamer, 1991). For the same pure protein-based system, increasing the heating pH to 6.9 or 7.1 caused increasing amounts of  $\kappa$ -casein dissociating from the CM into the serum, resulting in  $\kappa$ -casein–whey protein complexes in the serum and decreased levels of

CM covered with whey proteins (Daffner et al., 2020a). For concentrated milk systems after a heating step (120°C, 10 min), Singh & Creamer (1991) found that the dissociated protein was composed of 70%  $\kappa$ -casein, 20%  $\beta$ -casein and 10%  $\alpha$ -casein.

Other studies have not observed whey proteins on the surface of MFG, as occurred here, due to the difference in processing conditions, highlighting the potential for protein composition to be systematically altered. Only casein ( $\alpha$ ,  $\beta$  and  $\kappa$ ) and no whey or native membrane proteins (e.g. xanthinoxidase) were found on the surface of the MFG after homogenisation (Ong et al., 2010a), potentially due to low heating temperatures and a lack of denaturation of the whey proteins. Similarly, whey proteins were absent on the surface of the MFG after microfluidization, if the temperature was less than 70°C (Sharma & Dalgleish (1993).

Other processing variables appear to have less effect on the composition of proteins adsorbed to the MFG. Homogenisation pressure was found to have no effect on the composition of the proteins on the surface of the MFG, with 70% of the material characterised as casein and the rest being whey and native membrane proteins for all conditions examined (Cano-Ruiz & Richter, 1997). Sharma et al. (1996b) found the amount of  $\kappa$ -casein covering the surface of the MFG independent of the heat treatment performed and the order of the heating and homogenisation steps. They concluded that the deposition of  $\kappa$ -casein depended only on the homogenisation step. The  $\kappa$ -casein–whey protein complexes in the serum and on the MFG surface were proposed to be similar after heating and homogenisation (Sharma et al., 1996a).

Similar to the results of our work (compare *Table 1*), Sharma et al. (1996a) found increasing amounts of  $\alpha_s$ - and  $\beta$ -casein, but decreasing amounts of  $\kappa$ -casein and  $\beta$ -LG covering the surface of MFG after mechanical input, if the pH before a heating step was adjusted from 6.3 to 7.3, which also resulted in an increase in the casein to whey protein ratio from 4.62 (pH 6.3) to 8.01 (pH 7.3) on the surface of the MFG.

### 3.2 Rheological characterisation of sol–gel transition

The sol–gel transition temperatures ( $T_{\text{sol-gel}}$ ) of all formulations were determined with temperature sweeps at a heating rate of 1 K/min. The goal was to investigate the effect of additional dairy fat on the rheological behaviour of the protein-based systems (Daffner et al., 2020a).  $T_{\text{sol-gel}}$  of cold acidified casein–whey protein suspensions (8.0% (w/w) CS, 2.0% (w/w) WP) with added fat (to final fat contents of 1.0-, 2.5- and 5.0% (w/w)) after heating (pH 6.55, 6.9, 7.1) and mechanical input are shown in *Figure 6*. It was proposed that homogenised MFG can mimic the behaviour of CM and potentially coagulate in a manner similar to CM (Ji et al., 2016; Walstra & Jenness, 1984).

To enable comparison the behaviour of casein–whey protein suspensions without fat (Daffner et al., 2020a) was added as a baseline to all figures. The sol area lies below this line and the gel area above the line. The two most promising formulations using acidifications pH of 4.8 and 5.0, were chosen in the current study, based on previous studies (Daffner et al., 2020a; Nöbel et al., 2018), which reported more promising characteristics, including higher aggregation rates for these formulations, consistent with the desired application of 3D printing via the pH–T-route.

$T_{\text{sol-gel}}$  of casein–whey protein suspensions with fat after heating at pH 6.55 are illustrated in *Fig. 6 (A)*. Independent of the amount of fat, formulations showed lower values for the  $T_{\text{sol-gel}}$  with decreasing pH value (4.8 compared to 5.0), which was in accordance with results for casein–whey protein suspensions (Daffner et al., 2020) and casein-based systems (Nöbel et al., 2020). Apart from one sample (pH 5.0, 5.0% (w/w) fat content), higher  $T_{\text{sol-gel}}$  (2 – 5°C) were found. The more fat added, the closer the  $T_{\text{sol-gel}}$  were to those of formulations without any additional fat (*Fig. 6 (A)*). Increasing the heating pH (6.9) for formulations with fat resulted in lower  $T_{\text{sol-gel}}$  compared to results after a heating pH of 6.55 (*Fig. 6 (B)*). While 1.0- and 2.5% (w/w) of fat caused a slight increase in the  $T_{\text{sol-gel}}$ , a tendency to decreased values with 5.0%

(w/w) fat was found, independent of the acidification pH, which could potentially be explained with an increasing amount of particles per unit area capable to aggregate and form a gel.

The tendency to lower  $T_{\text{sol-gel}}$  with increased heating pH for casein–whey protein formulations with fat was further confirmed by results at a heating pH of 7.1. A decrease (2°C after addition of 1.0- and 2.5% (w/w) fat and more than 4°C after addition of 5.0% (w/w) fat) of  $T_{\text{sol-gel}}$  at an acidification pH of 5.0 compared to the formulation without any fat added is illustrated in *Fig. 6 (C)*. If these formulations (heating pH 7.1) were acidified to pH 4.8, pre-gelation characteristics ( $G' > 1$  Pa, where particles already started to aggregate before any heat-induced gelation) occurred, making them unsuitable for printing.

The decrease in  $T_{\text{sol-gel}}$  at higher heating pH is likely due to changes of the protein composition of the MFG membrane, shown via gel electrophoresis (compare *Fig. 5*). For acid gelation, 40% of the membrane had to be coated by serum proteins to significantly increase the storage modulus (Michalski et al., 2002b). In contrast to the finding of Hammelehle (1994) who did not find a shift in the coagulation after heating the formulations, our study showed significant changes in the  $T_{\text{sol-gel}}$  for protein-fat suspensions (8.0% (w/w) casein and 2.0% (w/w) whey protein), strongly dependent on the heating pH.

The results for  $T_{\text{sol-gel}}$  of formulations with 10.0% (w/w) casein and 2.5% (w/w) whey protein with additional fat are shown in *Fig. 6 (D)*. Due to the increased amount of protein plus additional fat, the overall total solid content increased. As a result, fewer formulations could be analysed and the results of formulations after a heating pH of 6.55 and 6.9 were summed up in one figure, which resulted in two coagulation lines. Pre-gelation ( $G' > 1$  Pa) was found for all formulations with a heating pH of 7.1 and no further analysis was conducted. A slight tendency to lower  $T_{\text{sol-gel}}$  at both heating pH values (6.55 and 6.9) was found for all formulations.

At this higher protein content and the lower acidification pH values of 4.8 and 5.0, the influence of additional fat on  $T_{\text{sol-gel}}$  was less distinct compared to results with the lower protein content.

Pre-gelation characteristics ( $G' > 1$  Pa) were found for several formulations after the addition of fat (e.g. pH 4.8, 5.0% (w/w) fat, heated pH 6.55 or pH 5.0,  $\geq 2.5\%$  (w/w) fat, heated pH 6.9), explained with the increase in the total solid content and a higher amount of particles per unit volume.

### **3.3 Aggregation rate of casein–whey protein suspensions mixed with milk fat**

As described in Daffner et al. (2020a), the aggregation rate (represented by the evolution of the  $G'$  after reaching the sol–gel transition temperature) of the formulations was used to analyse the aggregations kinetics of casein–whey protein suspensions mixed with fat. For a simplified comparison, a solid line was added in all images which represented the aggregation rate of pure protein-based suspensions. The horizontal dashed line for the aggregation rate was used as a positive indicator from printing tests towards future printing applications of casein–whey protein suspensions, if values of 250 Pa/ 10 K were exceeded (Daffner et al., 2020a).

The influence of three different amounts of fat on formulations with 8.0% (w/w) casein and 2.0% (w/w) whey protein followed by thermal (pH 6.55, 6.9 and 7.1) and mechanical energy input is shown in *Fig. 7 (A-C)*. Increased values for the aggregation rate (storage modulus  $G'$ ) with decreasing acidification pH (5.0 to 4.8) were found for formulations after a heating step at pH 6.55. If 1.0% (w/w) fat was added, independent of the acidification pH, the aggregation rate significantly decreased (47.7% at pH 5.0 and 29.0% at pH 4.8) compared to formulations without fat. While no change in  $G'$  was found after the addition of 2.5% (w/w) fat at acidification pH 4.8 and 5.0, the 5.0% (w/w) additional fat increased the values for the storage modulus  $G'$ , with maximum values of around 300 Pa at pH 4.8. The formulations with 2.5 and 5.0% (w/w) fat reached around 250 Pa/ 10 K for the aggregation rate and simple printing tests were conducted. As shown in *Fig. 7 (A)*, a stable and firm 3D-printed gel was only found for the formulation with 5.0% (w/w) fat at an acidification pH of 4.8, while the one at pH 5.0 (not shown) could not maintain the rectangular shape.

The results for the aggregation rate of the formulations after an increased heating pH of 6.9 and different amounts of fat added are illustrated in *Fig. 7 (B)*. The values for the storage modulus  $G'$  increased with decreasing acidification pH and increasingly amount of additional fat (one exception at pH 5.0 and 1.0% (w/w) fat content, with the highest increase in  $G'$  of 22.5% at pH 5.0 and 5.0% (w/w) fat. A significant increase of  $G'$  (heating pH 6.9) compared to formulations heated at lower pH (6.55) was demonstrated, evidenced by reaching or exceeding an aggregation rate of around 250 Pa/10 K for all formulations with milk fat addition. Although all formulations with fat addition showed promising aggregation rates after being heated at pH 6.9, only those acidified to pH 4.8 resulted in firm and very stable 3D-printed gels when heated during conveying (see printed gels related to aggregation rate in *Fig. 7 (B)*).

At a slightly alkaline heating pH of 7.1 and after the addition of fat, fewer casein–whey protein formulations could be analysed (see *Fig. 7 (C)*), as an acidification pH value of 4.8 resulted in pre-gelation characteristics ( $G' > 1$  Pa), preventing a temperature-triggered sol–gel transition. At an acidification pH of 5.0, a trend towards increased values of  $G'$  in samples with 1.0 and 2.5% (w/w) fat content was found, which became significant in the sample with 5.0% (w/w) fat content. All the formulations reached or exceeded an aggregation rate of 250 Pa/ 10 K with the highest value of  $325.9 \text{ Pa/ 10 K} \pm 18.3 \text{ Pa/ 10 K}$  (5.0% (w/w) fat). Independent of the amount of fat added, all three formulations, which were heated at pH 7.1 and cold acidified to pH 5.0, could be printed into small rectangular gels (*Fig. 7 (C)*). A linear increase in the gel firmness measured using penetration tests after addition of fat (2.0 – 10.0% (w/w) fat) to protein gels (4.3% (w/w)), manufactured via the pH–T-route, was found previously (Hammelehle, 1994). Such high fat contents could not be used in this study due to pre–gelation characteristics ( $G' > 1$  Pa) when the fat content of the samples was higher than 5.0% (w/w).

The influence of the addition of 1.0 and 2.5% (w/w) fat on the aggregation rate of formulations with an increased overall protein content of 12.5% (w/w), consisting of 10.0% (w/w) casein

and 2.5% (w/w) whey protein, followed by thermal (pH 6.55, 6.9) and mechanical input is shown in *Fig. 7 (D)*. Due to pre-gelation ( $G' > 1$  Pa) after the addition of fat at the higher protein content (total solid content increased), several samples could not be produced and no formulations with a heating pH of 7.1 was further investigated. This included the formulation with a heating pH of 6.55 and 5.0% (w/w) fat) which could not be further processed. The results of the aggregation rate of formulations after both heating pH values were combined in one figure (*Fig. 7 (D)*). At higher protein contents, a significant decrease in the storage modulus was demonstrated for all formulations after the addition of fat, independent of the heating pH and the acidification pH. This was proposed to be the result of the increased amount of total solids (fat and protein) in the same unit volume compared to formulations without any additional fat, therefore slowing down the aggregation kinetics of the protein particles, if an increase in the temperature (pH–T-route) triggered collision and gelation of the particles. All three formulations at this higher protein content were tested for printing and resulted in firm gels.

### **3.4 Tailored casein micelle and MFG surface characteristics towards printing applications**

Having applied the same thermal treatment (80°C, 10 min), CM with different composition and surface characteristics occurred, depending on the pH adjusted before heating to denature the whey proteins (Daffner et al., 2020a). The CM and protein subunits/ aggregates, which covered the MFG after thermal and mechanical treatment in this study, provided electrostatic and steric repulsion forces hindering coalescence of the fat particles. The small changes in the pH adjusted before heating allowed tailoring of the surface characteristics of the MFG, changing the sol–gel transition temperature (*Fig. 6*) as well as the aggregation rate (*Fig. 7*) of the protein suspensions mixed with fat compared to pure casein-whey protein based suspensions of our previous study (Daffner et al., 2020a). Therefore, the pH sensitive CM as well as the MFG covered with proteins reacted to changes in the acidification pH and contributed to the gelation process via the pH–T-route. A schematic illustration (*Fig. 8*) shows the effect of heating (80°C, 10 min) at the

three adjusted pH values (6.55, 6.9, 7.1) and a mechanical input (sonication and homogenisation at 500 bar) on the casein–whey protein suspensions mixed with dairy fat, as well as the proposed interactions between proteins and fat globules. Walstra & Jenness (1984) found that MFG after homogenisation could behave like CM and could be coagulated in the same way as pure proteins, although their experiment was conducted under resting conditions. In this study, the MFG, which were coated with different types of dairy proteins on the surface after mechanical input, showed a similar behaviour.

During high pressure homogenisation, CM adsorb faster to droplet surfaces than individual casein molecules (McClements, 2004). Results of the SDS-PAGE (*Fig. 5*) showed that  $\kappa$ -depleted CM (heating pH 7.1) covered the surface of MFG, which resulted in MFG more prone to aggregation compared to MFG covered with protein (CM with whey protein on the surface) after heating at pH 6.55, evidenced by lower  $T_{\text{sol-gel}}$  (compare *Fig. 6 (C)* to *(A)*). This was proposed to occur due to a decrease of the steric repulsion forces on the surface of the MFG covered with depleted CM, as parts of  $\kappa$ -casein dissociated into the serum which resulted in a less dense hairy layer protruding into the serum phase.

The different surface characteristics of the MFG after mechanical treatment changed the microstructure of protein-fat formulations. As the aggregation rate was used as a positive indicator towards printability with simple printing tests, not all formulations exceeding 250 Pa/ 10 K were found to result in firm and stable gels. We assume that MFG, which were heated at pH 6.55, were covered with CM, CM with whey protein on their surface as well as denatured whey protein aggregates, as shown from SDS-PAGE (*Fig. 5*). Those MFG were proposed to have stronger steric repulsion forces due to  $\kappa$ -casein on the outside of the CM, protruding into the serum. On the other hand, increased heating pH values (6.9, 7.1) resulted in  $\kappa$ -depleted CM which covered the MFG, demonstrated by a decrease of  $\kappa$ -casein found during SDS-PAGE (*Fig. 5*). It is assumed that this decrease in the amount of  $\kappa$ -casein on the outside of the casein



micelles and on the surface of the MFG caused lower steric repulsion forces, shown by higher aggregation rates of those formulations.

At a total protein content of 10.0% (w/w), consisting of 8.0% (w/w) casein and 2.0% (w/w) whey protein, only one formulation with additional fat after a heating pH of 6.55 was found to be printable. On the other hand, three formulations at each heating pH (6.9 and 7.1) could be printed, although a lower acidification pH 4.8 was necessary at heating pH 6.9. As CM were most depleted in  $\kappa$ -casein after being heated at pH 7.1 and therefore, steric repulsion forces of CM on their own and on the surface of MFG decreased, those formulations were the only ones being able to be printed at pH 5.0. The proposed interactions between protein and fat particles depending on the heating pH were schematically illustrated in *Fig. 8*. A similar increase of adsorbed caseins ( $\alpha_s$  and  $\beta$ ) with increasing heating pH value, but decreasing amounts of  $\kappa$ -casein and  $\beta$ -lactoglobulin were found elsewhere (Sharma et al., 1996a).

#### 4 Conclusion

The effect of dairy fat on casein–whey protein suspensions was characterised regarding the potential use for extrusion-based 3D-printing applications via the pH–T-route. Small fat particles in the nano metre range were mechanically produced and covered with different protein particles to mimic protein behavior during gelation. For promising formulations, sol–characteristics after cold acidification (pH 4.8/5.0), independent of the heating pH but dependent on the protein content, were evidenced by  $\zeta$ -potential ( $\sim -20$  mV) and rheology ( $G' = 0.1$  Pa) and a steep increase of  $G'$  above 1 Pa (sol–gel transition temperature) was found.

For protein-fat formulations heated at a lower pH (6.55) followed by mechanical input, an increase in the sol–gel transition temperature and a decrease in the aggregation rate, independent of the amount of fat added, was found. In contrast, a higher heating pH caused similar (pH 6.9) respectively lower (pH 7.1) sol–gel transition temperatures. For those higher heating pH values,

increased aggregation kinetics compared to casein–whey protein based suspensions without fat were found, resulting in more promising material characteristics ( $G' \geq 250$  Pa/ 10 K) for printing purposes. Dairy fat could thus be added to casein–whey protein suspensions which were considered to be printable via the pH–T-route, if the thermal and mechanical treatments tailored the material properties accordingly. Extrusion-based 3D-printing of protein-fat formulations inclusive a sol–gel transition was found to be more favourable at higher heating pH values.

## Acknowledgements

This work was supported by the Engineering and Physical Sciences Research Council [grant number EP/N024818/1]. This research was supported under Australian Research Council's Industrial Transformation Research Program (ITRP) funding scheme (project number IH120100005). The ARC Dairy Innovation Hub is a collaboration between The University of Melbourne, The University of Queensland and Dairy Innovation Australia Ltd. The authors would like to thank Ian Norton as well as Eddie Pelan for fruitful discussions and Adabelle Ong for help with the SDS-PAGE. The authors would like to thank The Bio21 Molecular Science & Biotechnology Institute at The University of Melbourne for access to equipment. Cryo EM was carried out at the Bio 21 Advanced Microscopy Facility, at The University of Melbourne. We acknowledge Unternehmensgruppe Theo Mueller for gifting the powders.

## References

- Aguilera, J. M., & Kessler, Hg. (1988). Physicochemical and rheological properties of milk-fat globules with modified membranes. *Milchwissenschaft* 43 (1988), 411-415.
- Buchheim, W. (1986). Membranes of milk fat globules ultrastructural biochemical and technological aspects. *Kieler Milchwirtschaftliche Forschungsberichte*, 38, 227-246.
- Cano-Ruiz, M. E., & Richter, R. L. (1997). Effect of homogenisation pressure on the milk fat globule membrane proteins. *Journal of Dairy Science*, 80(11), 2732-2739.

599 Cho, Y. H., Lucey, J. A., & Singh, H. (1999). Rheological properties of acid milk gels as af-  
600 fected by the nature of the fat globule surface material and heat treatment of milk. *International*  
601 *Dairy Journal*, 9(8), 537-545.

602 Daffner, K., Vadodaria, S., Ong, L., Nöbel, S., Gras, S., Norton, I., & Mills, T. (2020a). Design  
603 and characterization of casein-whey protein suspensions via the pH-temperature-route for ap-  
604 plication in extrusion-based 3D-Printing. *Food Hydrocolloids*, 105850.

605 Daffner, K., Hanssen, E., Norton, I. T., Mills, T., Ong, L., & Gras, G. L. (2020b). Imaging of  
606 dairy emulsions via a novel approach of cryogenic transmission electron microscopy using  
607 beam exposure. *Soft Matter*, 16(34), 7888-7892.

608 Dalglish, D. G. (1984). Measurement of electrophoretic mobilities and zeta-potentials of par-  
609 ticles from milk using laser Doppler electrophoresis. *Journal of Dairy Research*, 51(3), 425-  
610 438.

611 Derossi, A., Caporizzi, R., Azzollini, D., & Severini, C. (2018). Application of 3D printing for  
612 customized food. A case on the development of a fruit-based snack for children. *Journal of*  
613 *Food Engineering*, 220, 65-75.

614 Devnani, B., Ong, L., Kentish, S., & Gras, S. (2020). Heat induced denaturation, aggregation  
615 and gelation of almond proteins in skim and full fat almond milk. *Food Chemistry*, 126901.

616 Dickinson, E. (1994). Protein-stabilized emulsions. *Journal of Food Engineering*, 22, 59-74.

617 Dickinson, E. (1998). Rheology of emulsions - The relationship to structure and stability. In  
618 *Modern aspects of emulsion science* (pp. 145-174).

619 Dickinson, E. (1999). Caseins in emulsions: interfacial properties and interactions. *International*  
620 *Dairy Journal*, 9(3-6), 305-312.

621 Dickinson, E. (2012). Emulsion gels: The structuring of soft solids with protein-stabilized oil  
 622 droplets. *Food hydrocolloids*, 28(1), 224-241.

623 Godoi, F. C., Prakash, S., & Bhandari, B. R. (2016). 3d printing technologies applied for food  
 624 design: Status and prospects. *Journal of Food Engineering*, 179, 44-54.

625 Guinee, T. P., Gorry, C. B., O'Callaghan, D. J., O'Kennedy, B. T., O'Brie, N., & Fenelon, M.  
 626 A. (1997). The effects of composition and some processing treatments on the rennet coagulation  
 627 properties of milk. *International Journal of Dairy Technology*, 50(3), 99-106.

628 Hammelehle, B. (1994). Die Direktsaeuerung von Milch. Untersuchungen zur gezielten Ein-  
 629 flussnahme auf Textur und Konsistenz gesaeuerter Milchgel. PhD Thessis. Muenchen: Techni-  
 630 sche Universitaet Muenchen/ Weihenstephan.

631 Horne, D. S. (1998). Casein interactions: casting light on the black boxes, the structure in dairy  
 632 products. *International Dairy Journal*, 8(3), 171-177.

633 Huppertz, T., & Kelly, A. L. (2006). Physical chemistry of milk fat globules. In *Advanced*  
 634 *Dairy Chemistry Volume 2 Lipids* (pp. 173-212). Springer, Boston, MA.

635 Jacob, M., Schmidt, M., Jaros, D., & Rohm, H. (2011). Measurement of milk clotting activity  
 636 by rotational viscometry. *Journal of dairy research*, 78(2), 191-195.

637 Ji, Y. R., Lee, S. K., & Anema, S. G. (2016). Characterisation of heat-set milk protein gels.  
 638 *International dairy journal*, 54, 10-20.

639 Jørgensen, C. E., Abrahamsen, R. K., Rukke, E. O., Hoffmann, T. K., Johansen, A. G., & Skeie,  
 640 S. B. (2019). Processing of high-protein yoghurt—A review. *International Dairy Journal*, 88, 42-  
 641 59.

642 Kessler, H. G. (2002). Food and bio process engineering. *Dairy Technology*, 5th edition (Verlag  
 643 A. Kessler, Munich, Germany).

644 Lanaro, M., Forrestal, D. P., Scheurer, S., Slinger, D. J., Liao, S., Powell, S. K., & Woodruff,  
645 M. A. (2017). 3D printing complex chocolate objects: Platform design, optimization and eval-  
646 uation. *Journal of Food Engineering*, 215, 13-22.

647 Le Tohic, C., O'Sullivan, J. J., Drapala, K. P., Chartrin, V., Chan, T., Morrison, A. P., ... &  
648 Kelly, A. L. (2018). Effect of 3D printing on the structure and textural properties of pro-cessed  
649 cheese. *Journal of Food Engineering*, 220, 56-64.

650 Liu, W., Ye, A., Liu, W., Liu, C., & Singh, H. (2013). Stability during in vitro digestion of  
651 lactoferrin-loaded liposomes prepared from milk fat globule membrane-derived phospholipids.  
652 *Journal of dairy science*, 96(4), 2061-2070.

653 Lopez, C., Madec, M. N., & Jimenez-Flores, R. (2010). Lipid rafts in the bovine milk fat glob-  
654 ule membrane revealed by the lateral segregation of phospholipids and heterogeneous distribu-  
655 tion of glycoproteins. *Food Chemistry*, 120(1), 22-33.

656 Malone, E., & Lipson, H. (2007). Fab@ Home: the personal desktop fabricator kit. *Rapid Pro-*  
657 *totyping Journal*.

658 McClements, D. J. (2004). Protein-stabilized emulsions. *Current opinion in colloid & interface*  
659 *science*, 9(5), 305-313.

660 Michalski, M. C., Michel, F., Sainmont, D., & Briard, V. (2002a). Apparent  $\zeta$ -potential as a  
661 tool to assess mechanical damages to the milk fat globule membrane. *Colloids and Surfaces B:*  
662 *Biointerfaces*, 23(1), 23-30.

663 Michalski, M. C., Cariou, R., Michel, F., & Garnier, C. (2002b). Native vs. damaged milk fat  
664 globules: membrane properties affect the viscoelasticity of milk gels. *Journal of Dairy Science*,  
665 85(10), 2451-2461.

666 Michalski, M. C., Michel, F., & Geneste, C., (2002c). Appearance of submicronic particles in  
667 the milk fat globule size distribution upon mechanical treatments. *Le Lait*, 82(2), 193-208.

668 Mulder, H., & Walstra, P. (1974). *The milk fat globule* (p. 163). Farnham Royal: Common-  
669 wealth Agricultural Bureaux.

670 Nöbel, S., Seifert, B., Schäfer, J., Daffner, K., & Hinrichs, J. (2018). Oral presentation Food  
671 Colloids, Leeds 2018 - Session - Processing of Novel Structures for Functionality. Tempera-  
672 ture-triggered gelation of milk concentrates applied to 3D food printing.

673 Nöbel, S., Seifert, B., Daffner, K., Schäfer, J., & Hinrichs, J. (2020). Instantaneous gelation of  
674 acid milk gels via customized temperature-time profiles: Screening of concentration and pH  
675 suitable for temperature triggered gelation towards 3D-printing. *Food Hydrocolloids*, 106450.

676 Ong, L., Dagastine, R. R., Kentish, S. E., & Gras, S. L., 2010a. The effect of milk processing  
677 on the microstructure of the milk fat globule and rennet induced gel observed using confocal  
678 laser scanning microscopy. *Journal of food science*, 75(3), E135-E145.

679 Ong, L., Dagastine, R. R., Kentish, S. E., & Gras, S. L. (2010b). Transmission electron micros-  
680 copy imaging of the microstructure of milk in cheddar cheese production under different pro-  
681 cessing conditions. *Australian Journal of Dairy Technology*, 65(3), 222.

682 Rajagopalan, R., & Hiemenz, P. C. (1997). *Principles of colloid and surface chemistry*. Marcel  
683 Dekker, New-York, 8247, 8.

684 Roefs, P. F. M. (1986). *Structure of acid casein gels: A study of gels formed after acidification*  
685 *in the cold* (Doctoral dissertation, Roefs). Wageningen University & Research Centre.

686 Ross, M. M., Kelly, A. L., & Crowley, S. V. (2019). Potential Applications of Dairy Products,  
687 Ingredients and Formulations in 3D Printing. In *Fundamentals of 3D Food Printing and Appli-*  
688 *cations* (pp. 175-206). Academic Press.

689 Schäfer, J., Läufle, I., Schmidt, C., Atamer, Z., Nöbel, S., Sonne, A., Kohlus, R. & Hinrichs, J.  
690 (2018). The sol–gel transition temperature of skim milk concentrated by microfiltration as af-  
691 fected by pH and protein content. *International journal of dairy technology*, 71(3), 585-592.

692 Sharma, S. K., & Dalgleish, D. G., (1993). Interactions between milk serum proteins and syn-  
693 thetic fat globule membrane during heating of homogenized whole milk. *Journal of Agricultural*  
694 *and Food Chemistry*, 41(9), 1407-1412.

695 Sharma, R., Singh, H., & Taylor, M. W. (1996a). Recombined milk: factors affecting the pro-  
696 tein coverage and composition of fat globule surface layers. *Australian journal of dairy tech-*  
697 *nology*, 51(1), 12.

698 Sharma, R., Singh, H., & Taylor, M. W. (1996b). Composition and structure of fat globule  
699 surface layers in recombined milk. *Journal of Food Science*, 61(1), 28-32.

700 Singh, H., & Creamer, L. K. (1991). Influence of concentration of milk solids on the dissocia-  
701 tion of micellar  $\kappa$ -casein on heating reconstituted milk at 120° C. *Journal of dairy research*,  
702 58(1), 99-105.

703 Van Vliet, T., & Dentener-Kikkert, A. (1982). Influence of the composition of the milk fat  
704 globule membrane in the rheological properties of acid milk gels. *Netherlands Milk and Dairy*  
705 *Journal*, 36, 261-265.

706 Van Vliet, T., 1988. Rheological properties of filled gels. Influence of filler matrix interaction.  
707 *Colloid and Polymer Science*, 266(6), 518-524.

708 Walstra, P., & Jenness, R. (1984). *Dairy chemistry & physics*. John Wiley & Sons. New York.

709 Walstra, P., Wouters, J. T. M., & Geurts, T. J. (2006). *Dairy science and technology*. Boca  
710 Raton, FL, USA: CRC Press.

711 Wegrzyn, T. F., Golding, M., & Archer, R. H. (2012). Food Layered Manufacture: A new pro-  
712 cess for constructing solid foods. *Trends in Food Science & Technology*, 27(2), 66-72.

713 Ye, A., Singh, H., Taylor, M. W., & Anema, S. (2002). Characterization of protein components  
714 of natural and heat-treated milk fat globule membranes. *International Dairy Journal*, 12(4), 393-  
715 402.

716 Ye, A., Anema, S. G., & Singh, H. (2008). Changes in the surface protein of the fat globules  
717 during homogenisation and heat treatment of concentrated milk. *Journal of dairy research*,  
718 75(3), 347-353.



## Table Caption

**Table 1.** Proportions of individual proteins covering the milk fat globule surface after thermal (80°C, 10 min; pH adjusted to 6.55, 6.9 and 7.1) and mechanical treatment (sonication and homogenisation).

## Figure Captions

**Fig. 1.** Changes in the zeta-potential as a function of the pH of a micellar casein–whey protein suspensions (8.0% (w/w) CS, 2.0% (w/w) WP) mixed with dairy fat (to 1.0% (w/w) total fat), heated at pH 6.55 (●), at pH 6.9 (▲) and at pH 7.1 (Δ). For comparison, the zeta-potential of non-heated micellar casein (○) without any fat is shown. The casein to whey protein ratio was 4:1.

**Fig. 2.** Particle size distribution of casein–whey protein suspensions mixed with different amounts of fat to a total fat concentration of 1.0% (w/w), 2.5% (w/w) or 5.0% (w/w) after a heating step at pH 6.55 (a), 6.9 (b) or 7.1 (c) with either no mechanical input (●/red) or sonication/homogenisation at 500 bar (1.0% (w/w) fat = ○/blue hollow circle; 2.5% (w/w) fat = ▲/yellow triangle; 5.0% (w/w) fat = ■/green square). The inset graphs in all images focus on the particle size distribution of each formulation between 1 – 1000 nm to better see differences as a result of the addition of fat.

**Fig. 3.** CLSM micrographs of casein–whey protein suspensions mixed with milk fat (to a total fat of 2.5% (w/w)) and then thermally (80°C, 10 min, pH 7.1) and mechanically (sonication + homogenisation) treated. Samples were stained with FCF fast green and Nile red fluorescent dyes (fat appears as red and protein as green) as seen on the left. The image after deconvolution with Huygens software is shown on the right. The scale bars are each 5 µm in length.

**Fig. 4** Cryo-EM images of casein–whey protein (8.0% (w/w) CS and 2.0% (w/w) WP) suspensions with 2.5 % (w/w) milk fat that have been thermally (80°C, 10 min; adjusted pH 6.55/6/9/7.1) and mechanically (sonication and homogenisation at 500 bar) treated. Samples received a constant dose (5.72 e<sup>-</sup>/Å s) but an increasing dose time (moving left to right across the Figure, with the sample after the highest dosage appearing on the far right). A dilution of 1:10 with deionised water was used prior to analysis. The scale bar is 500 nm in length in all images. The increasing contrast between protein and fat particles as a function of exposure was used to differentiate between these two types of particles.

**Fig. 5.** SDS-PAGE analysis of proteins covering the milk fat globule surface membrane after thermal (80°C, 10 min) and mechanical treatment. A total fat content of 2.5% (w/w) was analysed for each sample. The molecular weight ladder (kDa) is shown on the left; Lane I-II: heated, pH 6.55; Lane III-IV: heated, pH 6.9; Lane V-VI: heated, pH 7.1.

**Fig. 6.** Sol–gel transition temperatures of cold acidified casein–whey protein suspensions (8.0% (w/w) CS and 2.0% (w/w) WP) with different amounts of milk fat added (to final fat contents of 1.0% (●), 2.5% (Δ), 5.0% (▲) and 0% (w/w) as comparison (○)) after heating at pH 6.55 (A), 6.9 (B) and 7.1 (C) and cold acidified casein–whey protein suspensions (10.0% (w/w) CS and 2.5% (w/w) WP) with different amounts of fat added after heating at pH 6.55 and 6.9 (D). A heating rate of 1 K min/min was applied.

**Fig. 7.** Aggregation rate (Pa/ 10K) of heated samples (80°C, 10 min, pH 6.55 (A), 6.9 (B) and 7.1 (C)) with constant protein content (8.0% (w/w) CS and 2.0% (w/w) WP) and with higher protein content (10.0% (w/w) CS and 2.5% (w/w) WP, (D)) at different pH values (4.8 – 5.2) with different amounts of fat added (to final fat contents of 1.0, 2.5 and 5.0% (w/w)) at 10°C after/higher than sol–gel transition temperature obtained by temperature sweeps with a heating rate of 1 K/min. The solid line in all images represents the aggregation rate of pure protein-based formulations and is added to simplify comparisons to protein–fat suspensions. The dotted line indicates the threshold where above 250 Pa/10 K the aggregation rate was used as a positive indicator towards printability in a simple printing tests as shown by images of the printed samples.

**Fig. 8.** Schematic presentation depicting the preparation of casein–whey protein suspensions mixed with milk fat for extrusion-based 3D-printing via the pH–T-route. After a thermal (80°C, 10 min, pH 6.55/ 6.9/ 7.1) and mechanical energy input, the newly created MFG membrane surface is covered by different types of proteins or protein subunits/ aggregates.

780 **Supplementary Fig. 1.** Optical microscopy of a casein–whey protein suspension inclusive  
781 added fat with native milk fat globules without any mechanical treatment (100x magnification).  
782 Big particles all represent milk fat globules. Scale bar = 5  $\mu\text{m}$  and 10  $\mu\text{m}$ .

Figure 1

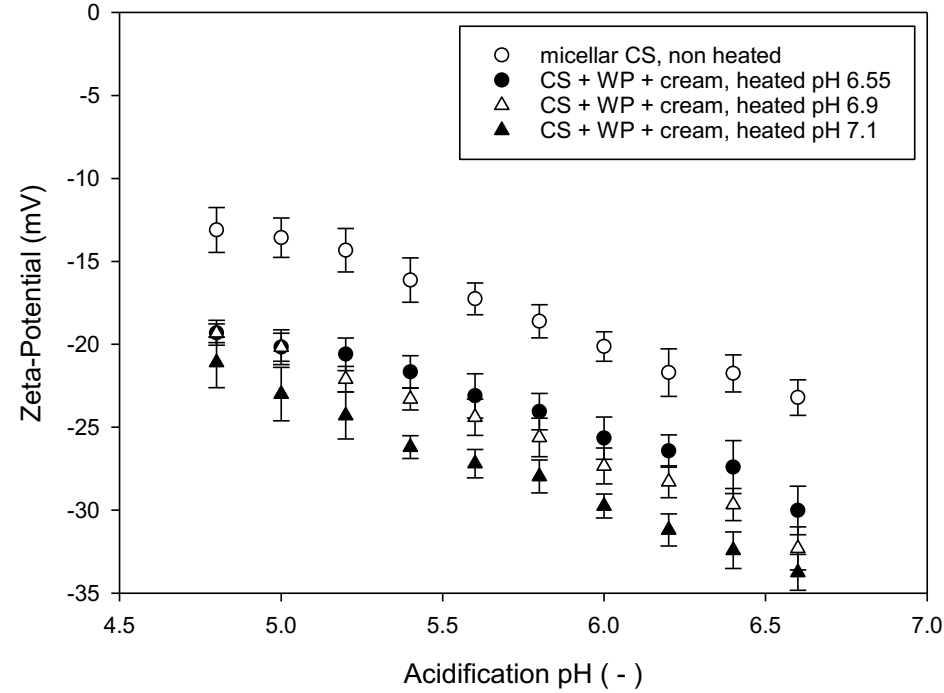


Figure 2

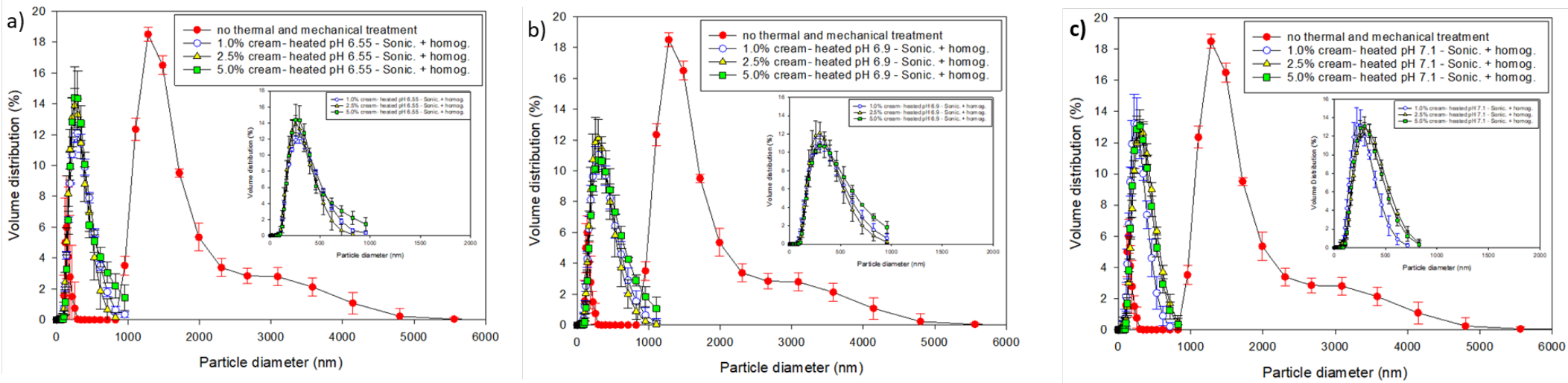


Figure 3

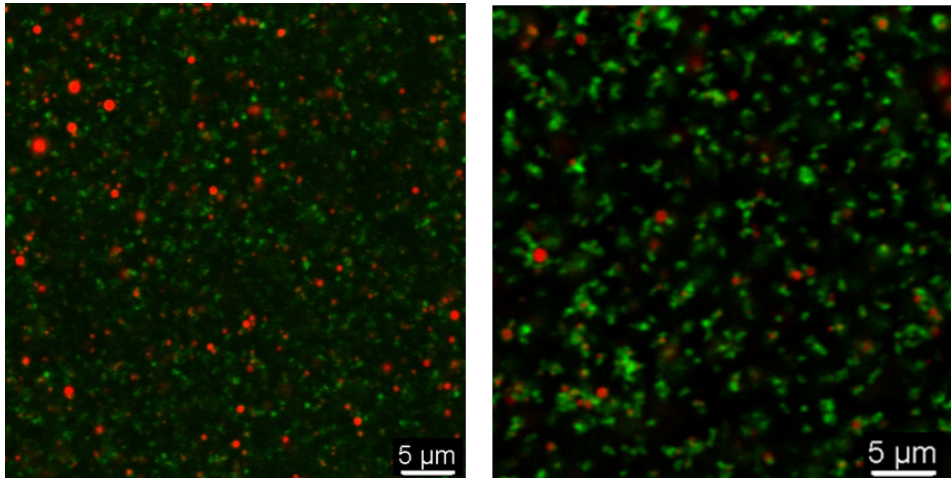


Figure 4

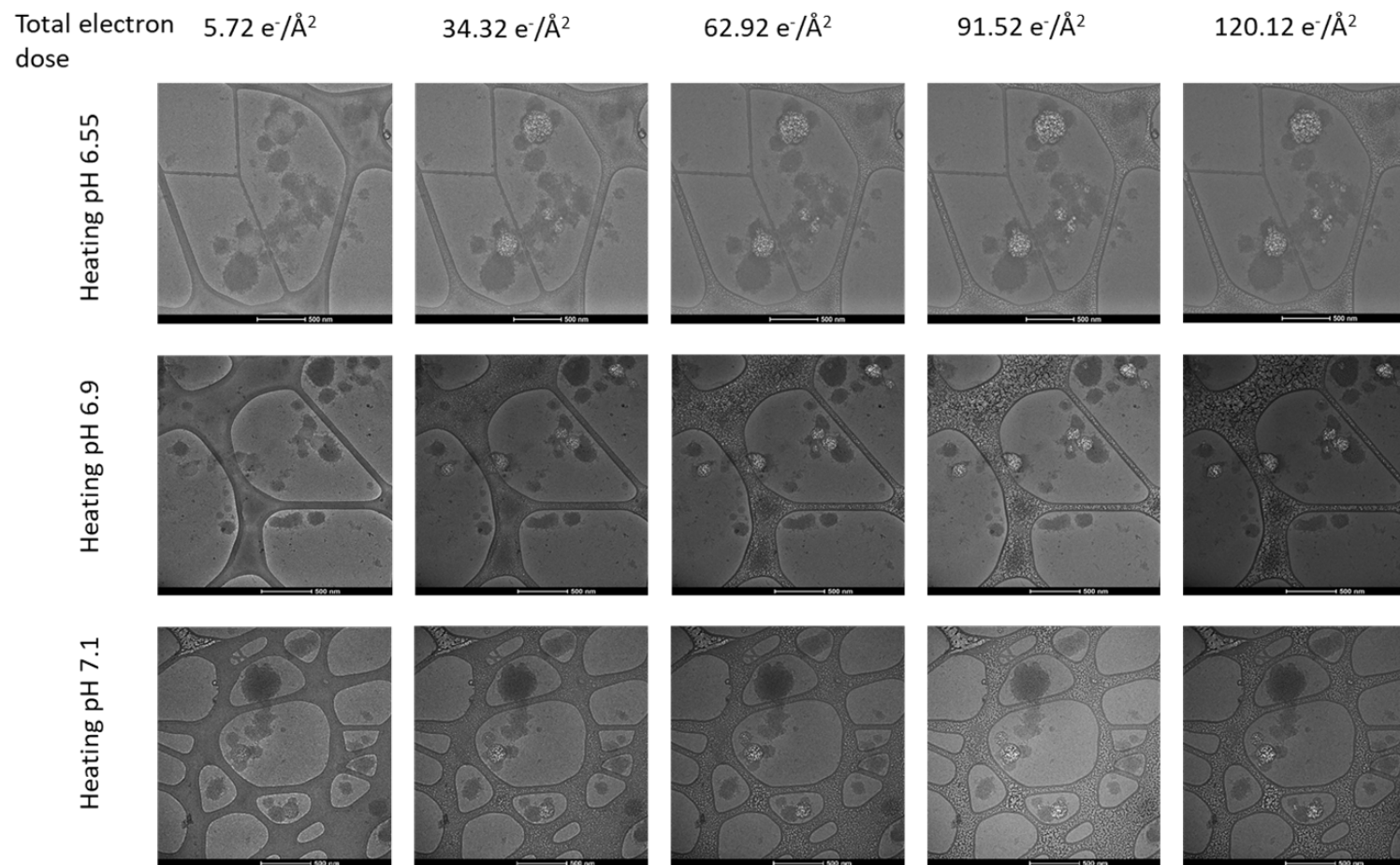




Figure 5

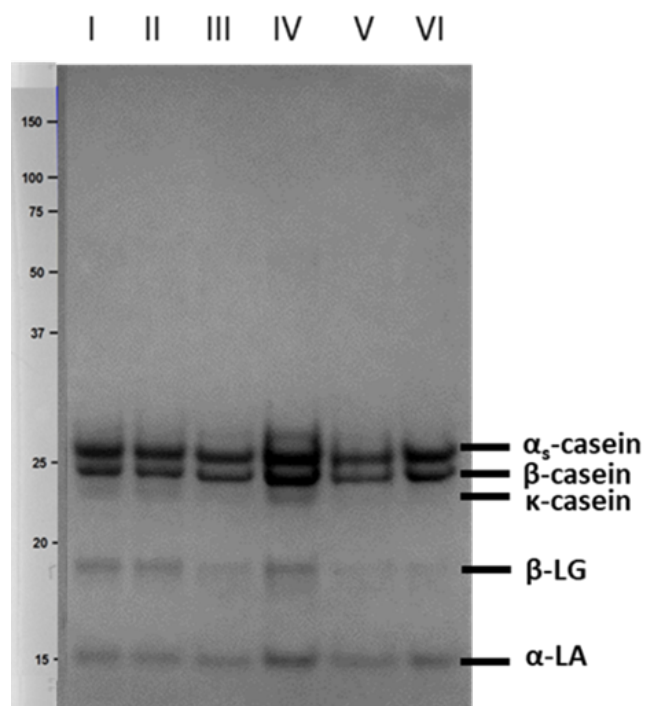


Figure 6

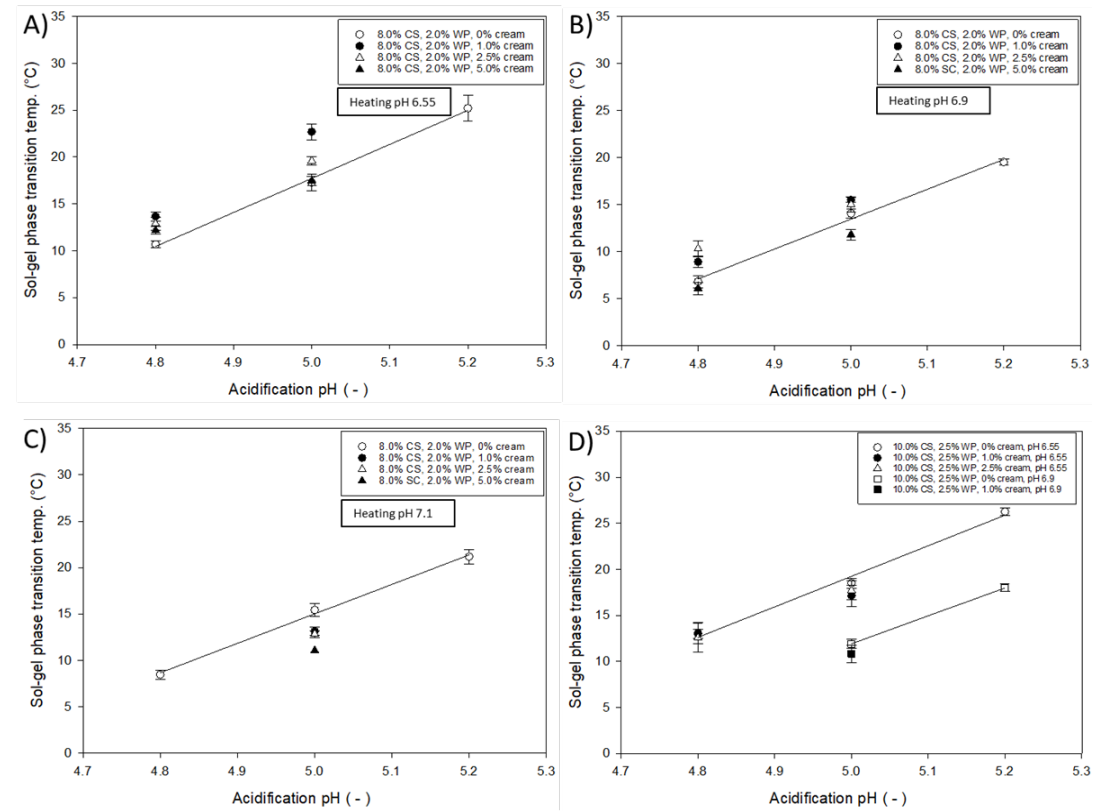


Figure 7

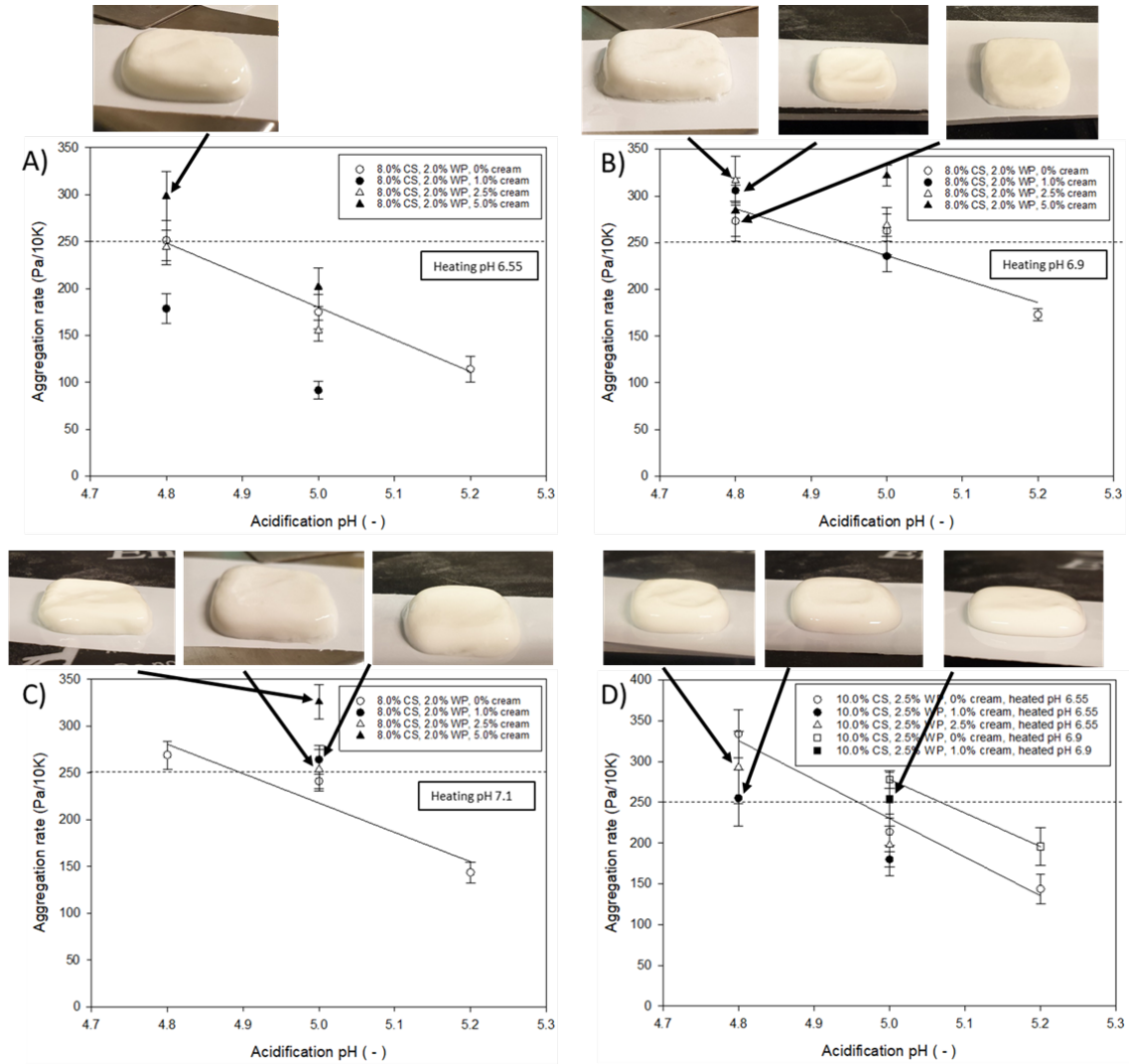


Figure 8

